

## COMPUTATIONAL EVALUATION OF THE EFFECT OF SOME THERMOLITHOGRAPHY PROCESS PARAMETERS ON RAPID PROTOTYPING

Rezende, R. A.\*, Andrade, S. R., Jardini, A. L., Scarparo, M.A.F., Maciel Filho, R.

*Chemical Engineering School, State University of Campinas (UNICAMP)  
Cidade Universitária Zeferino Vaz, CP 6066,  
CEP 13087-970 Campinas-SP, Brazil  
\* rezende@feq.unicamp.br*

**Abstract:** Reproducing physically three-dimensional virtual objects with free geometry by computer assistance translates what Rapid Prototyping (RP) is. Infrared Thermolithography (IRTL), a new RP method based on CO<sub>2</sub> laser irradiation onto thermosensitive resins, is presented. Their most important advantages are sample's non-contraction effect after curing and absence of post cure treatment. Localized cure consists on confining energy from laser beam to cure only the desired zone at resin and it is obtained in a best way from the combination of the physical parameters of IRTL process, as laser beam scanning speed and diameter. Simulations were performed with Ansys Software by Finite Element analysis based on the presented Numerical Model. *Copyright © 2007 IFAC*

**Keywords:** Rapid Prototyping, Thermolithography, Infrared Laser, IRTL Process, Simulation, Ansys, Thermosensitive Resin.

### 1. INTRODUCTION

Rapid prototyping (RP), also known as solid freeform fabrication or layer manufacturing, is a technology that fabricates models and prototype parts from geometric computer data. Unlike conventional machining, which involves removal of material, RP builds parts by selectively adding material layer by layer. The layers are obtained by converting a 3D CAD model into thin parallel slices bounded by their contours. With the RP technology, a part can be produced directly from the CAD data much faster than conventional methods (Wenbin, 2005). Many cases can present difficulties in producing models because of the contraction suffered by the prototype and of the additional treatment of post-curing, besides the high cost of equipments and materials used. Due to these reasons and difficulties, a process applying infrared laser was originated in Brazil at the School of Mechanical Engineering of State University of Campinas. The initial phase consisted on the production of small three-dimensional pieces with no contraction and eliminating the post-curing extra treatment (Scarparo *et al.*, 1992; Barros, 1993). Traditionally, the Stereolithography (SL), the eldest technique of Rapid Prototyping, marketed by 3D

System organization, is executed using an ultraviolet laser with application on special photosensitive resins. On the other hand, the Infrared Thermolithography (IRTL) process operates with the application of a CO<sub>2</sub> infrared laser. The used materials suffer reaction by the stimulus of temperature variation, since they are thermosensitives.

### 2. THE THERMOLITHOGRAPHY (IRTL) PROCESS

The Thermolithography Process, differently of SL process, works with thermosensitive resins. The prototypes show good spatial resolution, do not need post-cure treatment, absence of contraction, benefiting the localized cure and final shape of the projected object, besides high mechanical stiffness. The employed laser is CO<sub>2</sub> type with wavelength ( $\lambda$ ) equals to 10.6 $\mu$ m.

In Laboratory of Optimization, Process and Advanced Control (LOPCA) at School of Chemical Engineering at Unicamp is installed an IRTL system (see Figure 1).

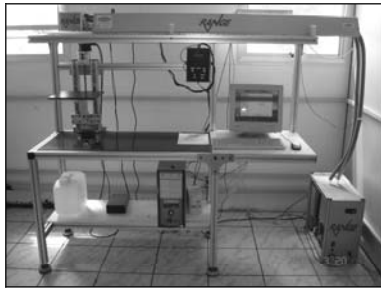


Fig. 1. IRTL machine at LOPCA.

The localized cure is the physical process where occurs a set of chemical reactions that provoke changes on the physical properties of the sample (normally from a liquid onto a solid material) by reacting of heat, catalyst and cure agents, isolated or on combining, with or without pressure (Bohm and Tveekrem, 1982; Billmeyer, 1984; Mano, 1985).

The localized cure consists on the solidification, at the right proportion, only in the region of the polymeric sample irradiated by the laser beam comprehended within the area defined by the beam diameter with an optical absorption depth  $\delta$  in the resin, generating a reached volume. This is the main subject of any process of stereolithography, either IRTL or SL. The present study is focused on obtainment of the best values for each variable in the process, more suitable for each condition.

So many are the parameters involved in a Rapid Prototyping system and, further more, the effects produced by the variations of those parameters, which require circumstantial analyses. The external temperature is one of the fundamental parameters in the resin cure process on the systems that operate with CO<sub>2</sub> laser.

The standard sample used in this paper is composed by a mixture of epoxy resin, diethylenetriamine and silica. The amount of silica in the sample is essential for the success of resin confinement (cure) under laser action. The silica function is to moderate the heat flux control, called *heat sink*. The materials and their respective proportions adopted are showed in Table 1 (Scarparo *et al.*, 1994).

Table 1 Sample composition and amounts.

Component	Proportion
Epoxy Resin (DGEBA)	100
Diethylenetriamine (DETA)	14
Silica powder	7

The proportion of silica in the sample changes the absorption depth of the resin. Then, silica is really another important issue to be taken into account in Thermolithography process (Rezende, 2006).

### 2.1 Computer Assistance Engineering on IRTL

CAE (Computer Aided Engineering) and CAM (Computer Aided Manufacturing) systems are complementary tools to the CAD (Computer Aided Design) ones. CAE provides numerical simulations and adjustments on direction to physical analyses of the model in terms of its engineering aspects, such as mechanicals and thermals, for instance. CAM offers analyses focused on the manufacturing phase that

embraces the system control, including all the decisions during the execution. In summary, allows generating the machining trajectories.

The CAD/CAM technologies have as function to model and to produce the pieces while Virtual Prototyping (CAE) has been used to help on simulating of the physical behavior on those pieces (Beaman *et al.*, 1997). At this project phase, there is no intention in simulating the physical behavior of the final product, but the polymeric material reaction (resin and reagents) during the cure process by laser.

In the last years, computational tools CAE have been developed for the support on problems of various engineering sectors through application of numerical methods.

### 2.2 Simulator – The Ansys Software

The Ansys software is a computational and mathematical CAE tool for analyses by finite element method of engineering problems in general. This is a powerful commercial software of simulation and it is extremely rich on resources for treatments of issues in areas such as thermodynamic (heat transfer, cooling effects, temperature gradients, thermal responses) and structure analyses (vibration, stress analyses, elasticity). The choice by Ansys, beside these resources, is because of the possibility of importing digital models for simulations (Ferreira *et al.*, 2001).

In this paper, a theoretical model developed for the reproduction in virtual environment (computational simulation) was used as reason and source to the Ansys, according to can be evidenced in the next section. The model contains the equations that govern the heat transference problem in the material, an overview about the involved parameters in the process and the contour conditions that are applied and analyzed (Scarparo *et al.*, 1992).

### 2.3 Numerical Model

This section describes how is implemented the Numerical Model to be submitted to Ansys program. Ansys is a tool based on the Finite Element Analysis. The equations relate mathematically the physical concepts of the Thermolithography process during the irradiation exposure on the polymeric sample. For the infrared CO<sub>2</sub> laser source simulation a term of heat generation constant was calculated in function of the laser power and the reached bulk. This irradiated bulk is obtained in term of the optical absorption depth and that is also dependent on the amount of silica in the sample.

A simple model to describe the flow of energy in laser-induced curing was constructed to predict both localization and curing rates as a function of laser parameters such as power, beam diameter, and scanning speed.

By the ratio between the beam diameter  $2\omega$  and the scanning speed  $v$ , one obtains the dwell time  $\tau_d$ ,

$$\tau_d = \frac{2\omega}{v} \quad (1)$$

which is the average time any spot on the laser scanning path is irradiated.

In order to predict the effect that the laser has on curing, we had to determine how much energy was delivered to the sample and over what volume that energy was distributed. Because the sample is highly absorptive at the CO<sub>2</sub> laser wavelength, nearly all of the energy in the beam during the dwell time is absorbed by the sample within a distance from the surface equal to the absorption depth  $\delta$ . The absorption depth was determined by measuring the transmittance of sample of uncured material over a wavelength range which included that of the CO<sub>2</sub> laser at 10.6 microns. Small cylindrical volume  $V$ , was assumed, that a absorbed an energy  $E$  during the dwell time, where  $V$  is given by (Equation 2)

$$V = \pi \cdot \omega^2 \cdot \delta \quad (2)$$

and  $\omega$  is the  $1/e$  radius of the laser beam.

The energy deposited in volume  $V$  is the product of the laser power and the dwell time (Equation 3)

$$E = P \cdot \tau_d \quad (3)$$

The approximation of Eq. (2) is reasonable for the sample in our experiment because the absorption depth is quite short. When working with a material which does not absorb the laser energy as strongly, the absorption depth may exceed the depth of focus of the laser beam. For such low-absorption cases, it is likely that the depth of focus will be the factor which best determines the confinement of laser energy in the direction normal to the sample surface. For the short irradiation times utilized in the previous experiments, the change in temperature,  $\Delta T$ , is directly proportional to the energy deposited through the heat capacity  $C_p$  and the mass  $m$  of the material contained in the volume  $V$  according to

$$E_p = C_p \cdot m \cdot \Delta T \quad (4)$$

To calculate the mass of the heated volume was used the mass density  $\rho = 1.16 \text{ g/cm}^3$ . Once the curing process is described as a function of temperature and time, the curing behavior can be predict as a function of laser irradiation conditions. Intuitively, if the laser is scanned too quickly over the sample, not achieve curing at all because any one spot does not absorb sufficient energy to initiate curing. When the scanning speed is to slow, the deposited energy would spread outward from the irradiated area and a larger area than desired would be cured.

The heat transfer is analyzed as a conduction problem, and the laser radiation is tacked into account as a heat source. The equation governing the conduction of heat can be derived from the principle of energy conservation and it can be written as (Equation 5):

$$\rho c_p \left( \frac{\partial T}{\partial t} + V_x \frac{\partial T}{\partial x} + V_y \frac{\partial T}{\partial y} + V_z \frac{\partial T}{\partial z} \right) = \ddot{q} + \frac{\partial}{\partial x} \left( k_x \frac{\partial T}{\partial x} \right) + \frac{\partial}{\partial y} \left( k_y \frac{\partial T}{\partial y} \right) + \frac{\partial}{\partial z} \left( k_z \frac{\partial T}{\partial z} \right) \quad (5)$$

where  $T$  is the temperature of sample,  $\rho$  is the density,  $c_p$  is the specific heat,  $k$  is the material conductivity,  $V$  is the velocity for transport of heat,  $q$  is the heat generation rate per unit volume. The amount of heat in the sample due to the laser beam scanning is taking into account in this heat generation term. The value of heat generation, is this model, is consider depending on laser power and volume irradiated as shown in Equation 6:

$$\ddot{q} = \frac{P}{\pi \omega^2 \delta} \exp \left( -\frac{r^2}{\omega^2} - \frac{|z|}{\delta} \right) \quad (6)$$

where  $P$  is the laser power,  $\omega$  is radius of the laser beam and  $\delta$  is the absorption depth,  $r$  is the distance of the center of the beam,  $z$  is the depth from surface of the sample. It has already been discussed that this parameter ( $\delta$ ) depends on amount of silica and its values has been showed by Figure 2.

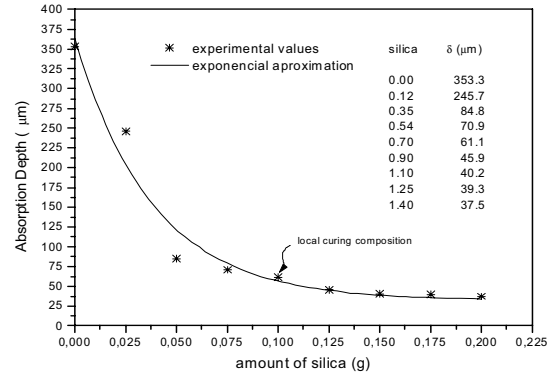


Fig. 2. Absorption depth in terms of amount silica.

As initial condition, it is considered room temperature (25°C) at the sample and air. At interface between sample and air occurs conduction of heat.

### 3. RESULTS

The temperature is the mandatory parameter in Thermolithography process. The localized cure is determined by the analysis of the temperature around the irradiated area on the resin. The numerical model as could be seen is extremely approached by the temperature effect.

The localized cure occurs by energy transference through the entire sample from an initial laser beam radiation. Some aspects are important to be analyzed such as laser operational parameters as so the sample physical properties. The analysis showed in this paper shows the influence of the laser beam scanning speed and the laser beam diameter. The simulations executed with Ansys present the temperature sample behaviors at the center and edge of the material. The geometry regarded in the simulations represents a

transversal cut of a rectangular area of the sample (see Figure 3), in contact with air, under laser beam exposure. The physical properties values of the sample and the air region are related in Table 2.

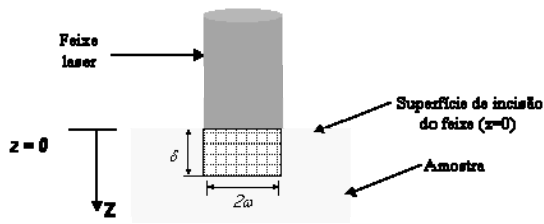


Fig. 3. Laser beam and dimensions.

Table 2 Standard Physical Properties of the Sample.

Physical Properties	Sample	Air	Absorption Depth $\delta$
Thermal Conductivity (W/mK)	0.0427	0.026	60 $\mu\text{m}$
Mass Density (Kg/m <sup>3</sup> )	2799	1,16	
Specific Heat (J/KgK)	1383	1007	

For the first group of simulations were considered the two following values for the scanning speed of the laser beam ( $v$ ): 1.60 m/s and 2.39 m/s. The diameter has a fixed value of  $d=0,8\text{mm}$ .

For the second group, the diameters ( $d$ ) simulated were: 0.6mm, 0.8mm, 1.0mm and 1.2mm with fixed speed of scanning equals to  $v=1.60\text{m/s}$ .

### 3.1 First group: Effect of laser beam scanning speed

The diameter of laser beam is  $d = 0.8\text{mm}$ , where this value corresponds to the real laser beam used in experimental performances at lab, and the Laser Beam Power is  $P = 20\text{W}$ , in all the simulated cases (see figures 4 up to 8).

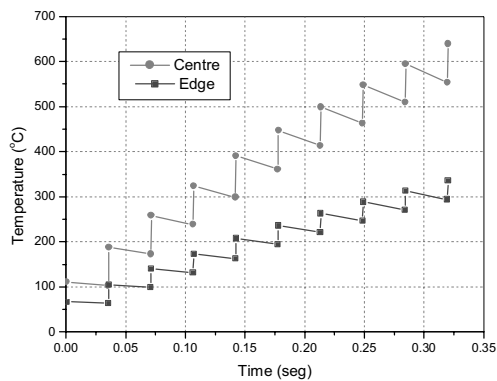


Fig. 4. Temperature Profile of surface (at center and edge) after 10 pulses for  $v = 1.60$  m/s.

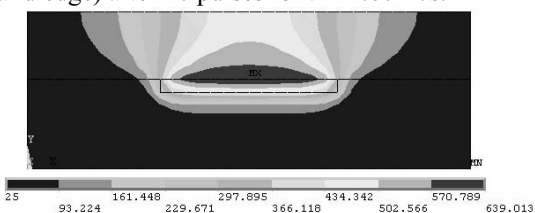


Fig. 5. Isothermal Profile after 10 pulses ( $v = 1.60$  m/s).

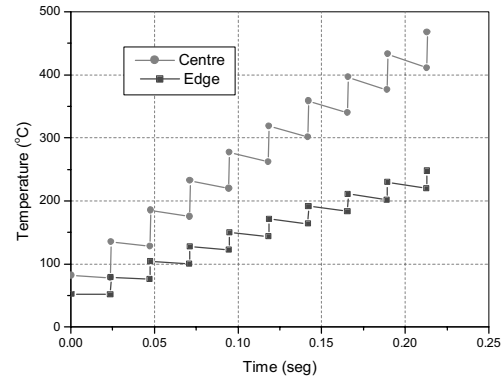


Fig. 6. Temperature Profile of surface (at center and edge) after 10 pulses for  $v = 2.39$  m/s.

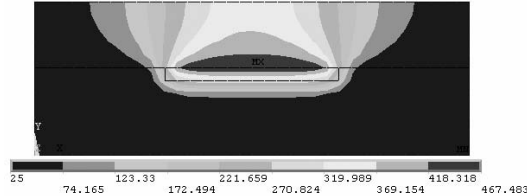


Fig. 7. Isothermal Profile after 10 pulses ( $v = 2.39$  m/s).

The final temperature values of the simulations can be found graphically in Table 3 for the center and edge positions at the sample.

Table 3 Values of final temperatures on resin surface (after 10 pulses) at center and edge for “ $d$ ” variation

Figure	Variable analyzed Velocity (m/s)	Maximum temperatures °C (after 10 pulses) Center	Edge	Difference Center – Edge (°C)
4-5	1.60	639.0	335.7	303.3
6-7	2.39	467.5	247.5	220.0

### 3.2 Second group: Effect of laser beam diameter

The diameter  $d$  of laser beam is now varied. The laser beam power is  $P = 20\text{W}$ , in all the simulated cases are  $d=0.6\text{mm}$ ,  $d=0.8\text{mm}$ ,  $d = 1.0\text{mm}$  and  $d = 1.2\text{mm}$ . The results can be seen in Figures 8 up to 16.

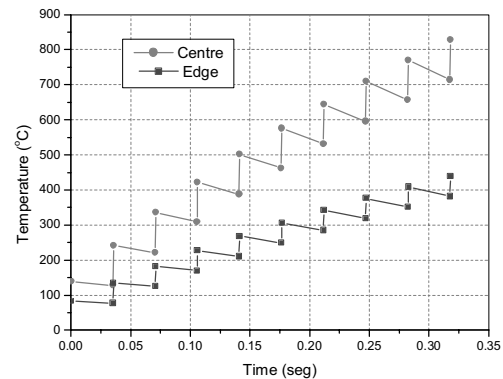


Fig. 8. Temperature Profile of surface (at center and edge) after 10 pulses ( $d=0.6\text{mm}$ ).

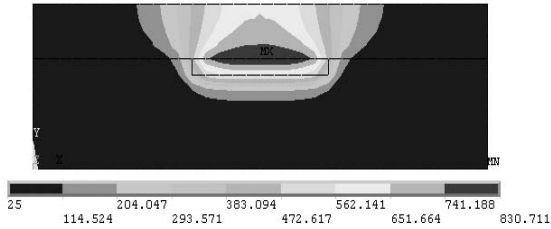


Fig. 9. Isothermal Profile after 10 pulses (d=0.6mm).

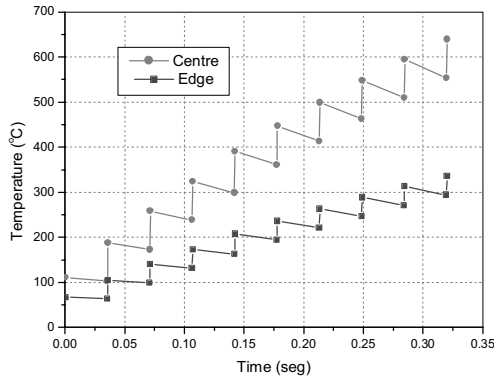


Fig. 10. Temperature Profile of surface (at center and edge) after 10 pulses (d=0.8mm).

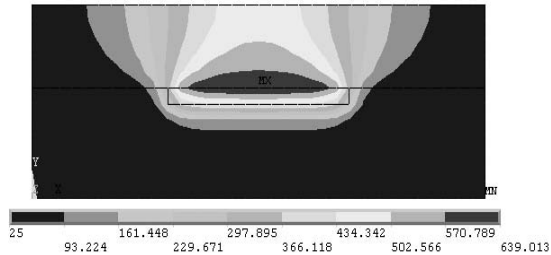


Fig. 11. Isothermal Profile after 10 pulses (d=0.8mm).

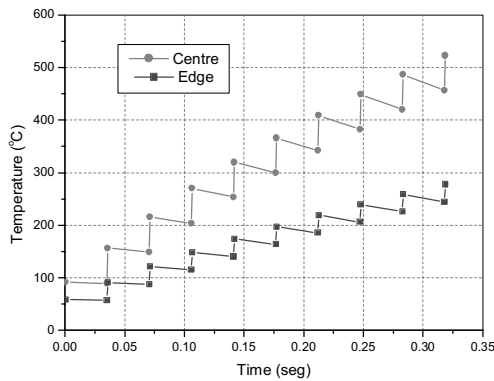


Fig. 12. Temperature Profile of surface (at center and edge) after 10 pulses (d=1.0mm).

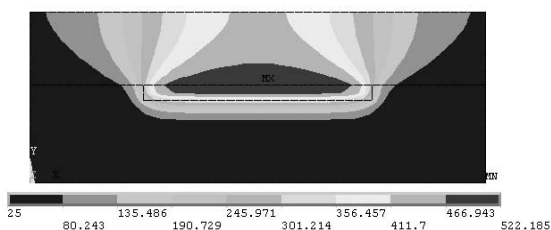


Fig. 13. Isothermal Profile after 10 pulses (d=1.0mm).

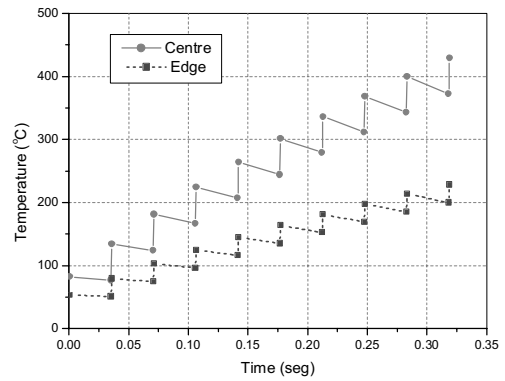


Fig. 14. Temperature Profile of surface (at center and edge) after 10 pulses (d=1.2mm).

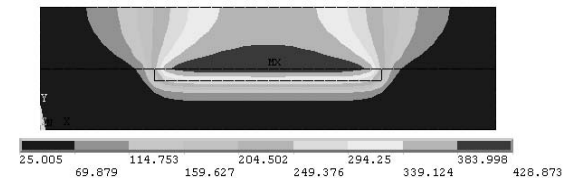


Fig. 15. Isothermal Profile after 10 pulses (d=1.2mm).

Table 4 Values of final temperatures on resin surface (after 10 pulses) at centre and edge for “v” variation

Figure	Variable analyzed Diameter (mm)	Maximum temperatures °C (after 10 pulses)		Difference Center – Edge (°C)
		Center	Edge	
8-9	0.6	827.8	439.6	388.2
10-11	0.8	639.0	335.7	303.3
12-13	1.0	522.2	277.4	244.8
14-15	1.2	428.7	228.4	200.3

The calculated temperature numbers in Table 3 and 4 are essential to comprehend the behaviour in the resin sample after IR irradiation and also to have a better control during next experimental works.

The figures depicting the profile of temperature spreading at surface are very friendly to illustrate the energy concentration in the sample after the last pulse. It eases to perceive what is the effective cured region, that is, if the localized cure occurs within the region bounded by the laser beam and how much energy reaches further the edge.

#### 4. CONCLUSIONS

The results obtained by simulations show that with the scanning speed of laser beam variation, the final temperatures at center and edge of the polymeric sample also varied after 10 pulses of irradiation. As much the speed is increased, the temperatures at center and edge decrease. Further, increasing the speed implicates a faster irradiation over a specific point which means lower values of temperatures and therefore lower differences of temperature between center and edge. The dwell-time in case of figures 4-

5 is equivalent to 503  $\mu\text{s}$  and for figures 6-7 equals to 334  $\mu\text{s}$ . In figure 4-5, after the first pulse, the difference of temperature achieved between the centre and edge is about 44 °C. After the last pulse (10<sup>th</sup>) the difference goes to 303 °C. In figure 6-7, the simulation showed, for the first pulse, the difference of 29 °C while the last pulse showed 220 °C. The variation of the scanning speed of the two Cases 4-5 and 6-7, after the ten pulses, leads to a decrease medium of 26.5% of their temperatures from the first to the second case.

For the diameter simulations, as much the diameter is increased the temperatures at center and edge decrease. Further, the increasing of diameter implicates to a larger distance for the spreading of the irradiated energy that means lower values of temperatures at the edge and therefore lower differences of temperature between center and edge. One pulse has a duration time of 35.33ms (dwell-time) being that 34.95ms correspond to a cooling time and the 38 $\mu\text{s}$  correspond to the effective time of exposure under the laser beam irradiation. The heating time is about 100 times lower than the cooling one that helps to assure the integrity. Further this, the degradation temperature for this sample is equals to 277°C, obtained through measures performed from the gravimetric process.

Because of the low thermal conductivity of the sample, each radiation of the site results is essentially adiabatic, rise in the temperature which does not decay to ambient between irradiations. The temporal behavior of the temperature of an irradiated site would be a series of temperature spikes on a constant background with a decay time equal to the cycle time (repetition rate). Because of the simplifying assumption of temperature independent thermal properties each adiabatic temperature spikes is about the same, in each considered real case. Temperature profile across sample-air interface after about 10 pulses shows various curves of a range of temperatures (isotherms): it is possible to compare the size of the central isotherm with the size of the laser beam, and it figured out that they are nearly identical ( $1/e$  of  $T_{\text{max}}$ ) (Andrade *et al.*, 2005).

#### ACKNOWLEDGMENTS

The authors would like to thanks for the support by FAPESP and CAPES.

#### REFERENCES

- Andrade, S.R., Jardini, A.L., Rezende, R.A., Maciel Filho, R. and Scarparo, M.A.F. (2005). Heat Sink Silica Effect: A New Approach Using Ansys Program Simulation in Thermal Stereolithography (TSTL) Process. *Proceedings of the 2<sup>ND</sup> International Conference on Advanced Research in Virtual and Rapid Prototyping*, **28**, 519-525, September-October, Leiria, Portugal.
- Barros, M.L. (1993). Estudo, Desenvolvimento e Obtenção de Peças Plásticas Tridimensionais através da Litografia Térmica com Laser de CO<sub>2</sub>, *Master thesis*, School of Chemical Engineering, State University of Campinas.
- Beaman, J.J., Marcus H.L., Bourel, D.L., Barlow, J.W. and Crawford, R.H. (1997). *Solid Freeform Fabrication: A New Direction in Manufacturing*, Kluwer Academic Publishers. Dordrecht London.
- Billmeyer, F.W. (1984). *Textbook of Polymer Science*, John Wiley & Sons, 3<sup>a</sup> ed., New York.
- Bohm, G.G. and Tveekrem, J. (1982). *Rubber Chemical Technological*, **55**, 575.
- Ferreira, J.M.G., Alves, N.M.F., Mateus, A.J.S. and Custódio, P.M.C. (2001). Desenvolvimento Integrado de Produtos e Ferramentas por Metodologias de Engenharia Inversa e Técnicas de Prototipagem Rápida, *3<sup>o</sup> Congresso Brasileiro de Gestão de Desenvolvimento de Produto*, 25-27 Setembro, Florianópolis. Santa Catarina.
- Mano, E.B. (1985) *Introdução a Polimeros*, Ed. Edgard Blucher Ltda, 111p, São Paulo.
- Rezende, R. A. (2006). Análises de Parâmetros Físicos e Operacionais no Fenômeno da Cura Localizada do Processo Termolitográfico da Prototipagem Rápida. *Master thesis*, School of Chemical Engineering, State University of Campinas.
- Scarparo, M.A.F., Barros, M.L. and Gerck, E. (1992) Estereolitografia a Laser. Uma Nova Técnica. *Anais do V Simpósio Estadual de Lasers e Aplicações*.
- Scarparo, M.A.F., Barros, M.L., Gerck, E., Kiel, A. and Hurtack, J.J. (1994). Stereolithography with Thermosensitive Resins using a CO<sub>2</sub> Laser, *Journal of Applied Polymer Science*, **54**, 1575-1578.
- Wenbin, H., Tsui, L. Y. and Haiqing, G. (2005). A study of the staircase effect induced by material shrinkage in rapid prototyping. *Rapid Prototyping Journal*, **11**, 2, 82-89.